Simulation of the electrical transient during the porous anodizing of pure aluminium substrate

F. Le Coz, L. Arurault & R. S. Bes
CIRIMAT-LCMIE, Université Paul Sabatier, Toulouse, France

Abstract

Electrical transients were recorded during the anodizing of highly pure aluminium in phosphoric electrolyte, carried out in potentiostatic mode (25-150V) or in galvanostatic conditions (20-1000A/m^2). The experimental reproductibility is satisfactory, according to the low standard deviations.

For the galvanostatic mode, the voltage experimental transients show a "bell shape", characterized by some significant parameters (S_0, t_m, V_m, V_{ss}). Two mathematical relations were then proposed to simulate the voltage transient curves considering two parts, i.e. before and after the maximum (V_m, t_m). The validity of these computational simulations was next checked by comparison with the corresponding experimental curves. All the corresponding fittings of voltage transients are in good agreement, especially for the first part of the experimental curves, within the current densities range.

Then, these computational simulations were correlated with the corresponding experimental FEG-SEM plan-views. By analogy with the nucleation phenomena during the metal electrodeposition, the "bell shaped" curves could be interpreted by the initial formation of a highly resistive oxide layer, followed by the subsequent appearance of the nanopores. The pores formation was in part explained showing that the V_m experimental values obtained with the galvanostatic mode are closed to the previous critical voltage value U_c initializing the anodic dissolution phenomenon.

Keywords: electrical transients, anodic film, simulation, nanopores, anodizing.

1   Introduction

Anodizing of aluminium and its alloys is an established electrochemical process, discovered in 1855 by H. Buff and developed in 1911 by De Saint Martin.

Industrially, it rapidly acquired great importance due to the various applications (against corrosion, decoration…) in different fields like aeronautic, architecture, etc. About twenty years ago, there was a renewal of interest for this process due to the possibility, in special operational conditions, to obtain highly nano-ordered templates based on the Anodic Aluminium Oxide (AAO) [1,2]. Moreover, recent research works [3-5] showed that a later impregnation of metal or oxide, followed by the removal of the AAO matrix, allowed to prepare nano-objects, like plots or wires, of which the sizes depend directly on the previous geometrical characteristics of the AAO nanopores. The porous anodic film growth on aluminium substrates in general, and the self-nanostructuring of the AAO templates in particular, is still today considered to be a complex phenomenon, until now not well understood in spite of the wide range of academic experimental studies. But the previous research works experimentally show for example the great importance of the surface pretreatments and of the initial electrical transients of anodizing to prepare convenient AAO templates.

From this point of view, despite previous preliminary works [6-10], further efforts are necessary to explain the initial electrical transients obtained either under galvanostatic anodizing mode or in potentiostatic anodizing conditions, as well as to correlate simultaneously these electrical transients with the surface nanoporosity of the aluminium substrates.

The aim of this study is to develop mathematical relations simulating the electrical transients during the anodizing of highly pure aluminium in acidic electrolyte, thereby extending our previous works [11,12] about the control of the initial surface state and of the final nanoporosity characteristics of the anodic film. In particular, these computational simulations will be compared to the corresponding experimental measurements, and correlated with the nanoporosity using FEG-SEM views of the aluminium substrates.

2   Experimental

The substrate material is highly pure aluminium (99.99%Al). The aluminium sheets (0.1x40x40mm) were first degreased for one minute in an aqueous alkaline bath containing NaOH (5g/L), $Na_2CO_3,6H_2O$ (5g/L), $Na_3PO_4,12H_2O$ (10g/L), $Na_2SiO_3,5H_2O$ (1g/L) and $NaC_6H_{11}O_7$ (10g/L), then etched in aqueous NaOH (25g/L) for one minute and neutralised in aqueous HNO_3 (20%v/v) for 2 minutes. Each step was conducted at ambient temperature, and the samples were rinsed in distilled water.

The aluminium sheet was then used as anode and a lead plate (3x40x40mm) as counter-electrode in a cell regulated at $-1.5°C$. The electrolyte was made up of an aqueous motionless H_3PO_4 (8%wt) solution. All chemical were analytical grade products (PROLABO) and the aqueous solutions were prepared using deionized water.

The input direct current or voltage was imposed by a NEMIC LAMBA generator (GEN 300-5), while a potentiostat/galvanostat (PGP 201 TACUSSEL-RADIOMETER) controlled by a microcomputer was used to record the curves as a function of the time (U = f(t) or J = f(t) respectively).

The micro and nanostructures, especially of the porosity of the samples, were observed by Field Emission Gun Scanning Electron Microscope (FEG-SEM JEOL JSM 6700F).

3   Results and discussion

3.1 Potentiostatic anodizing mode

Figure 1 shows the electrical transients obtained under potentiostatic mode, i.e. at a constant potential drop (U) between the working and the counter-electrodes. This figure reveals two main types of curve shapes. The first one, obtained when U < 120V, is a decreasing curve whereas for higher voltages, the current density increases drastically with the time. In this second case, the anodizing process becomes rapidly out of control due to the high value of current density (>500 A/m^2), while the aluminium sample is rapidly damaged.
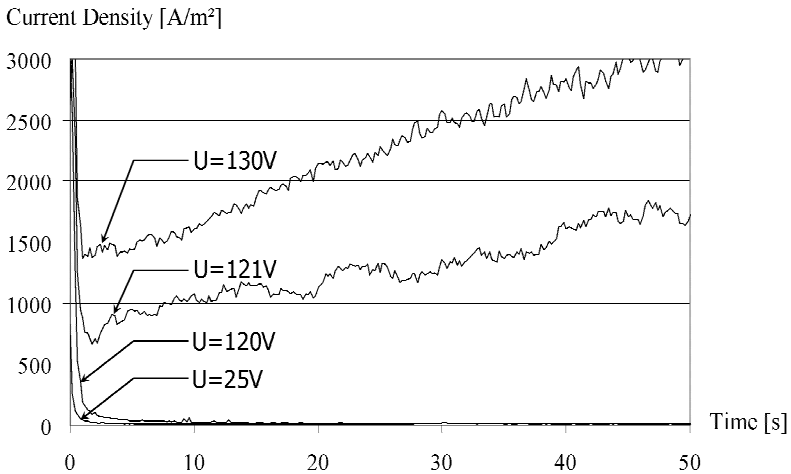

Figure 1:   Electrical transients obtained in potentiostatic mode (U=25V, 120V, 121V and 130V).

The critical voltage value (here U_c = 120V) distinguishes between two domains: the anodizing process (for $U < U_c$) and the anodic dissolution (for $U > U_c$). The anodizing in these operational conditions can be assimilated to a "hard anodizing" due to the use of a strong acid solution (pKa$_1$ = 2.05 at 0°C [13]) at a low temperature (–1.5°C), the resulting surface porosity being usually lower than 10% [14]. On the contrary, at higher voltages, the anodic dissolution induces the direct oxidation from the aluminium metal to the aluminic ion (Al^{3+}), preventing the formation of an anodic film and causing the sample damage.

3.2 Galvanostatic anodizing mode

3.2.1 Preliminary definitions

For the galvanostatic mode, the voltage evolution as a function of time shows qualitatively a "bell shaped" curve (Figure 2), characterised by some quantitative experimental data:

the initial slope of the voltage transient: $(dV/dt)_{t\to 0} = S_0$

the coordinates of the maximum: t_m and V_m

the steady-state voltage V_{ss} at $t = +\infty$

For the simulation, the transient voltage-time curves are considered as composed typically of two parts, i.e. before and after the maximum (V_m, t_m).
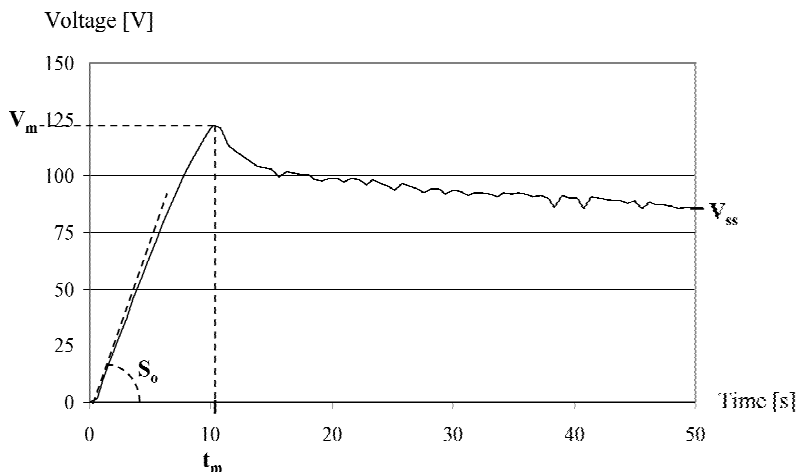

Figure 2:   Typical voltage transient obtained in galvanostatic mode ($J=300A/m^2$).

3.2.2 Reproductibility

Three voltage-time transients, obtained for strictly identical anodizing conditions ($300A/m^2$), show that the initial slope S_0 ($S_0 = 13.6\pm0.7V/s$), the maximum voltage V_m ($V_m = 122.3\pm0.3V$) and the maximum time t_m ($t_m = 10.5\pm0.3s$) remain constants, their relative deviations being less than 5%, while the steady state voltage V_{ss} varies by 11% ($V_{ss} = 85.8\pm9.3V$). According to the low standard deviations obtained, the experimental reproductibility is considered to be good.

3.2.3 Response before the maximum ($0 \le t \le t_m$)

At first, the initial slope S_0 was studied as a function of the current density J. The results clearly demonstrate that the initial slope is directly proportional to the current density (Figure 3).

By similarity with the previous work of Patermarakis et al [7], the following relation is now proposed to simulate the first part of the electrical transient, i.e. to the maximum voltage:

$$V(t) = P_0.t - P_1.t.\exp(\lambda_1.t) \qquad (0 \le t \le t_m) \qquad (1)$$

where P_0, P_1 and λ_1 are constants for a fixed value of the current density, under the considered anodizing conditions.

The derivative of this relation is:

$$(dV/dt) = P_0 - P_1.(\lambda_1.t + 1).\exp(\lambda_1.t) \qquad (2)$$

At $t \approx 0$, the initial slope is then:

$$(dV/dt)_{t\to 0} = S_0 = P_0 - P_1 \qquad (3)$$

The corresponding fits are in very good agreement with the experimental curves for current densities from 20 to 1000 A/m^2. As an example, Figure 4 shows the excellent fitting of the experimental transient obtained at 300 A/m^2, the values of P_0, P_1 and λ_1 being respectively 14.0V/s, 0.0001V/s and 0.98s^{-1}.
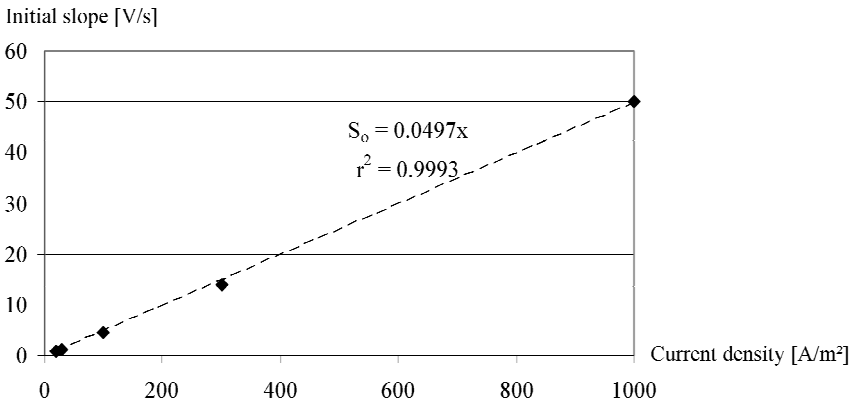

Figure 3: Evolution of the initial slope S_0 as a function of the current density J.
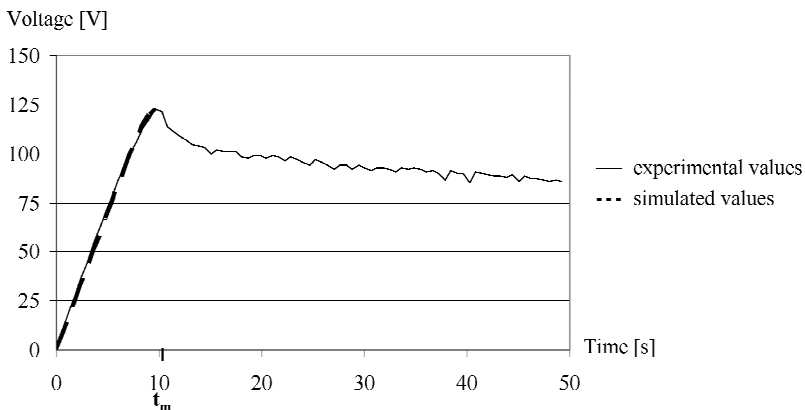

Figure 4: Fitting (for $t \le t_m$) of the experimental voltage transient (J = 300A/m^2).

3.2.4 Response after the maximum ($t_m \leq t < \infty$)

The relation used to fit the second part of the voltage transients in the 20 to 1000 A/m^2 range, is based on the previous works of Goad and Dignam [6] and Wu and Hebert [9,10]:

$$V(t) = V_{ss} + (V_0 - V_{ss}).\exp(-\lambda_2.t) \qquad (t_m \leq t < \infty) \qquad (4)$$

with $V_0 = S_0.t_m$ and λ_2 is a constant for a fixed value of the current density, under the considered anodizing conditions.

Figure 5 provides an example of the experimental transient obtained at 300 A/m^2 compared with the corresponding fitting curve ($\lambda_2 = 0.35s^{-1}$, $V_{ss} = 85.8V$ and $V_0 = 1284.1V$). In this second part, the fitting curve is closed to the experimental one apart from the first seconds after the maximum voltage V_m.
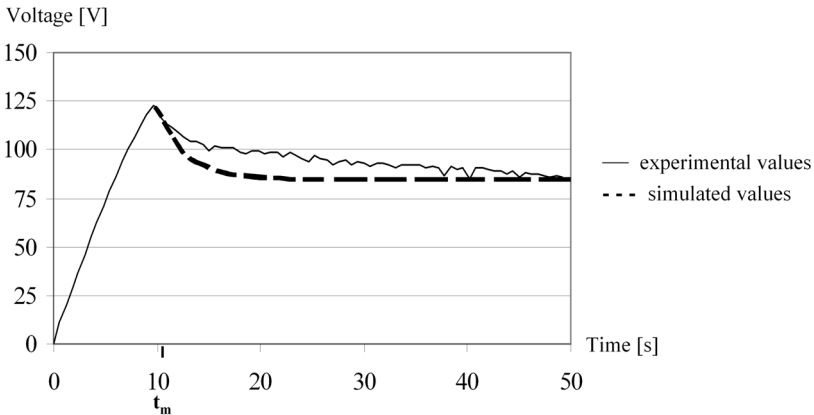

Figure 5:   Fitting (for $t \geq t_m$) of the experimental voltage transient ($J = 300$ A/m^2).

3.3 Electrical transients and materials

3.3.1 Theoretical considerations

While reduction mechanisms were extensively investigated [15,16], only few theoretical studies concern the oxidation, especially for chronopotentiometry on metallic electrode. The more usual case is the oxidation from ion to ion in solution (Red $\rightarrow$ Ox + ne) on an inert solid metallic electrode M_s, the electrode potential depending on the kinetic of the electronic transfer through a logarithm-type relation. Considering now the anodic dissolution, i.e. the oxidation of a solid metal electrode M_s to ion in solution M^{n+} ($M_s \rightarrow M^{n+} + ne$), the electrode potential is then given by:

$$E = E^0_{M^{n+}/M} + \left(\frac{RT}{nF}\right)\ln\left(\frac{2i\sqrt{t}}{nFS\sqrt{\pi D_{M^{n+}}}}\right) \quad for \ C^*_{M^{n+}} = 0 \qquad (5)$$

On the other hand, the case of an anodizing, from a solid metal M_s to a solid oxide MO_s appears more unusual, since this solid-solid oxidation includes also the incorporation of oxygen from the solvent. Moreover, the chemical

composition of the anodic layer is in fact complex, including various types of oxi-hydroxides, having a global electric behaviour of a semi-conductor [12]. Consequently, the two previous theoretical cases do not allow to explain the typical appearance of the experimental curves during the anodizing, specially the initial peak after galvanostatic polarisation (Figure 2).

By analogy, these typical "bell shaped" curves should be in fact very similar to the chronopotentiograms obtained during the nucleation phenomena in metal electrodeposition [17,18]. In that case, the initial potential increase is linked to the double-layer charge, while the decrease should be typical of a nucleation phenomenon. The crystallization overvoltage of this second phase of the peak was then expressed by:

$$\eta(t) = \eta_\infty - \eta_\infty \exp(-kt) \qquad (6)$$

where k is a constant and η_∞ is the difference between the electrode potentials respectively at t_∞ and t_m, time corresponding to the maximum value of the potential peak. The theoretical value of η_∞ is usually difficult to obtain because it directly depends of the faradic current i_F, whose value is not exactly known, due to the contribution of the current corresponding to the charge of the double layer. It is interesting to remark now that relation 6 is similar to the previous relation 4, suggesting similar phenomena. However, these phenomena cannot be rigorously compared because the time's scales are greatly different (lower than 0.5s for electrodeposition and higher than 40s for anodizing using low current density). So, it could be probably considered that, in the anodizing case, the initial voltage increase is only due for a weak part to the charge of double layer, and that another phenomenon predominates during the first part of the experimental curves.

3.3.2 Porosity

FEG-SEM plan views (Figure 6(a) and (b)) show that the nanoporosity appears on the sample surface as the function of the current density in the 20-1000 A/m² range. At low densities (Figure 6(a)), the surface is quasi-free of porosity while nanopores clearly emerge from the surface at higher density (Figure 6(b)). Other FEG-SEM views (not shown here) reveal similar facts when the anodizing time is increased at constant current density.
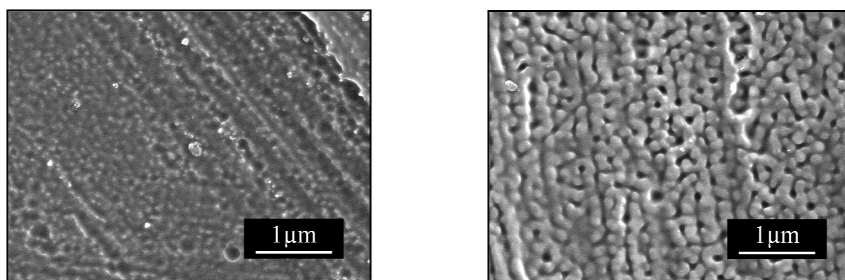

Figure 6:   FEG-SEM plan view of sample surface: (a) J=20A/m², (b) J=50A/m².

By analogy with the nucleation phenomena during the metal electrodeposition, the "bell shaped" curves could be interpreted in fact by the initial formation of the highly resistive oxide layer, called the "compact layer" or the "barrier layer", contributing for the main part to the initial voltage increase. The subsequent appearance of the nanopores, inducing then the voltage decrease, induces then preferential conducting points concentrating the current lines distribution, following by analogy the example of the metal initial adatoms during the nucleation phenomena in metal electrodeposition. From this point of view, it is interesting to note that for this anodizing the V_m experimental values obtained with the galvanostatic mode are closed to the previous critical voltage value U_c defining the start of the anodic dissolution in potentiostatic mode.

At the end of the "bell shaped" curve, the steady-state voltage V_{ss} depends simultaneously on both the growth of the anodic layer and its chemical dissolution by the strong acid solution. These explanations clearly show the great influence of the electro-chemical dissolutions in the second part of the curves. So the use of a motionless electrolyte probably induces the deviation of the steady-state voltage V_{ss}, as well as the differences between experimental and fitting curves during the first seconds after the maximum (V_m, t_m).

4   Conclusion

The aim of this study was to develop mathematical relations simulating the electrical transients during the anodizing of highly pure aluminium in phosphoric electrolyte under dc electrical conditions. Electrical transients were recorded during the anodizing carried out in potentiostatic mode (25-150V) or in galvanostatic conditions (20-1000 A/m^2).

The current transients obtained under potentiostatic mode reveal two main types of curve shapes. The first one is a decreasing curve, whereas for higher voltages, the current density increases drastically as a function of the time. A critical voltage value (U_c = 120V) separates the two domains: anodizing for $U < U_c$ and anodic dissolution for higher voltage values.

For the galvanostatic mode, the voltage experimental transients show a "bell shape", characterized by some significant parameters (S_0, t_m, V_m, V_{ss}). The experimental reproducibility was good, according to the low standard deviations apart from the steady-state voltage V_{ss}.

The transient voltage curves were simulated considering two domains (before and after the maximum at t_m) according to the following mathematical relations:

$$V(t) = P_0.t - P_1.t.\exp(\lambda_1.t) \qquad (0 \le t \le t_m)$$
$$V(t) = V_{ss} + (V_0 - V_{ss}).\exp(-\lambda_2.t) \qquad (t_m \le t < \infty)$$

where P_0, P_1, λ_1 and λ_2 are constants for a fixed value of the current density, under the considered anodizing conditions. All the corresponding fittings of voltage transients are in good agreement, especially for the first part of the curves, with the experimental curves for current densities in the 20 - 1000 A/m^2 range.

Then, these computational simulations were correlated with the corresponding experimental FEG-SEM plan-views. By analogy with the nucleation phenomena during the metal electrodeposition, the "bell shaped" curves could be explained by the initial formation of the highly resistive oxide layer, followed by the subsequent appearance of the nanopores, acting then like preferential conducting points concentrating the current lines distribution. The pores formation was in part explained showing that the V_m experimental values obtained with the galvanostatic mode are closed to the previous critical voltage value U_c.

So, this study developed convenient computational simulations in view to simulate and to predict the voltage transients in galvanostatic conditions, allowing finally control of the initial surface state and the nanoporosity characteristics of the anodic film. But now, additional experiments are required to understand the self-nanostructuring phenomenon involved in the preparation of the AAO templates.

References

[1]   Masuda H., Fukuda K., Ordered metal nanohole arrays made by a two-step replication of honeycomb structures of anodic alumina, *Science*, **268**, pp. 1466-68, 1995.

[2]   Jessensky O., Müller F., Gösele U., Self-organized formation of hexagonal pore arrays in anodic alumina, *Applied Physics Letters*, **72(10)**, pp. 1173-75, 1998.

[3]   Inoue S., Chu S-L., Wada K., Li D., Haneda H., New roots to formation of nanostructures on glass surface through anodic oxidation of sputtered aluminum, *Science and Technology of Advanced Materials*, **4**, pp. 269-276, 2003.

[4]   Hwang S-K., Lee J., Jeong S-H., Lee P-S., Lee K-H., Fabrication of carbon nanotube emitters in an anodic aluminium oxide nanotemplate on a Si wafer by multi-step anodization, *Nanotechnology*, **16(6)**, pp. 850-858, 2005.

[5]   Qin D-H., Zhang H-L., Xu C-L., Xu T., Li H-L., Magnetic domain structure in small diameter magnetic nanowire arrays, *Applied Surface Science*, **239**, pp. 279-284, 2005.

[6]   Goad D.G.W., Dignam M.J., Transient Response of the System Al/Al$_2$O$_3$/Electrolyte. Part I. Galvanostatic Transients, *Canadian Journal of Chemistry*, **50(20)**, pp.3259-3266, 1972.

[7]   Patermarakis G., Lenas P., Karavassilis C., Papayiannis G., Kinetics of growth of porous anodic Al$_2$O$_3$ films on A1 metal, *Electrochimica Acta*, **3**, pp. 709-725, 1991.

[8]   Parkhutik V.P., Shershulsky V.I., Theoretical modelling of porous oxide growth on aluminium, *J. Phys D: Appl. Phys.*, **25**, pp. 1258-1263, 1992.

[9]   Wu H., Hebert K.R., Electrochemical transients during the initial moments of anodic oxidation of aluminium, *Electrochimica Acta*, **47**, pp. 1373-1383, 2002.

[10]   Wu H., Hebert K.R., Reply to comments on « Electrochemical transients during the initial moments of anodic oxidation of aluminum », *Electrochimica Acta*, **48(2)**, pp. 131-133, 2002.

[11]   Zamora G., Arurault L., Bes R.S., Energetics of aluminium alloys anodization for porous oxide films elaboration, *Surface Treatment VI – Computer Methods and Experimental Measurements for Surface Treatment Effects*, ed. C.A. Brebbia, J.T.M. de Hosson and S.I. Nishida, WIT Press, Southampton, pp 51-59, 2003.

[12]   Zamora G., PhD Thesis, Paul Sabatier University, Toulouse France, 07/01/2005 (in French).

[13]   Weast R.C., Handbook of Chemistry and Physics, CRC Press, London, 1975-1976.

[14]   Gabe D.R., Density values for anodic films on aluminium and some observations of pore morphology, Trans IMF, **78(6)**, pp. 207-209, 2000.

[15]   Delahay P., Mamantov G., Voltammetry at constant current: Review of theoretical principles, *Anal. Chem.*, **27(4)**, pp. 478-83, 1955.

[16]   Reinmuth W. H., Chronopotentiometric Potential-Time Curves and Their Interpretation, *Anal.Chem.*, **32(11)**, pp. 1514-17, 1960.

[17]   Fleischmann M., Thirsk H.R., Anodic electrocrystallization, *Electrochimica Acta*, **2(1-3)**, pp. 22-49,1960.

[18]   Chamelot P., Lafage B., Taxil P., Studies of niobium electrocrystallization phenomena in molten fluorides, *J. Electrochem. Soc.*, **143(5)**, pp. 1570-1576, 1996.